



Published in final edited form as:

*Proc SPIE Int Soc Opt Eng.* 2015 February ; 9417: . doi:10.1117/12.2081418.

## Low dose dynamic myocardial CT perfusion using advanced iterative reconstruction

Brendan L. Eck<sup>1</sup>, Rachid Fahmi<sup>1</sup>, Christopher Fuqua<sup>1</sup>, Mani Vembar<sup>2</sup>, Amar Dhanantwari<sup>2</sup>, Hiram G. Bezerra<sup>3</sup>, David L. Wilson<sup>1</sup>

<sup>1</sup>Department of Biomedical Engineering, Case Western Reserve University, Cleveland, OH, 44106, USA

<sup>2</sup>Philips Healthcare, Cleveland, OH 44143, USA

<sup>3</sup>Cardiovascular Imaging Core Laboratory, Harrington Heart & Vascular Institute, University Hospitals Case Medical Center, Cleveland, OH, 44106, USA

### Abstract

Dynamic myocardial CT perfusion (CTP) can provide quantitative functional information for the assessment of coronary artery disease. However, x-ray dose in dynamic CTP is high, typically from 10mSv to >20mSv. We compared the dose reduction potential of advanced iterative reconstruction, Iterative Model Reconstruction (IMR, Philips Healthcare, Cleveland, Ohio) to hybrid iterative reconstruction (iDose<sup>4</sup>) and filtered back projection (FBP). Dynamic CTP scans were obtained using a porcine model with balloon-induced ischemia in the left anterior descending coronary artery to prescribed fractional flow reserve values. High dose dynamic CTP scans were acquired at 100kVp/100mAs with effective dose of 23mSv. Low dose scans at 75mAs, 50mAs, and 25mAs were simulated by adding x-ray quantum noise and detector electronic noise to the projection space data. Images were reconstructed with FBP, iDose<sup>4</sup>, and IMR at each dose level. Image quality in static CTP images was assessed by SNR and CNR. Blood flow was obtained using a dynamic CTP analysis pipeline and blood flow image quality was assessed using flow-SNR and flow-CNR. IMR showed highest static image quality according to SNR and CNR. Blood flow in FBP was increasingly over-estimated at reduced dose. Flow was more consistent for iDose<sup>4</sup> from 100mAs to 50mAs, but was over-estimated at 25mAs. IMR was most consistent from 100mAs to 25mAs. Static images and flow maps for 100mAs FBP, 50mAs iDose<sup>4</sup>, and 25mAs IMR showed comparable, clear ischemia, CNR, and flow-CNR values. These results suggest that IMR can enable dynamic CTP at significantly reduced dose, at 5.8mSv or 25% of the comparable 23mSv FBP protocol.

### Keywords

CT Perfusion; low dose CT; iterative reconstruction

## 1. INTRODUCTION

Computed Tomography (CT) is a vital imaging modality in today's clinical environment. CT serves a prominent role in the emergency department due to its ability to quickly deliver anatomical volumetric data for physician review. One example is the use of coronary CT

angiography (CCTA) for the noninvasive diagnosis of coronary artery disease [1]. CCTA is able to accurately detect severe coronary stenosis [2] but is unable to determine whether a moderate stenosis is physiologically significant [3]. Thus, noninvasive CT angiography is often paired with a functional exam such as SPECT cardiac perfusion, which is the current clinical standard [4]. SPECT perfusion requires a separate imaging exam from the CT evaluation, which increases diagnostic time and reduces patient throughput. With the addition of myocardial perfusion, CT could provide a one-stop diagnostic workflow for coronary artery disease yielding both anatomical and functional information, serving as an ideal gate keeper for invasive diagnostics.

Myocardial CTP has been under development for a number of years; however x-ray dose in these studies has been high. Previous reports [5, 6] have shown in patients that dynamic myocardial CTP can be used for the identification of ischemia, but technical challenges have prevented clinical adoption. To address such challenges, preclinical models have been used in the development and validation of perfusion quantification and artifact reduction techniques [7–10]. Despite these developments, the effective dose of protocols used in these studies remains high, ranging from 10mSv [6] to 24mSv [11]. Many dynamic CTP protocols have greater dose than the current clinical standard of SPECT perfusion, around 10mSv [12], which has been trending toward lower dose levels. To address the dose concern, hybrid iterative reconstruction (IR) algorithms have been able to reduce dose in many clinical cardiac applications [13, 14] as well as preclinical CTP cases [11, 15]. Advanced IR algorithms, which include CT system models and noise statistics, may be able to further reduce dose [16, 17] and motivate this study.

In this work, we evaluate the dose savings potential of an advanced IR (IMR) compared to hybrid IR (iDose<sup>4</sup>) and conventional FBP in both static and dynamic myocardial CT perfusion. We use a projection-based low dose simulation tool [18] to generate low dose CTP scans from physical high dose scans. This method enables direct comparison of the noise effects on CTP images at reduced dose independent of image artifacts or physiologic variation which may differ in physical scans. We compare the image quality of static CTP images and the image quality of blood flow maps from dynamic CTP processing at 100mAs, 75mAs, 50mAs, and 25mAs to find the dose reduction potential of advanced iterative reconstruction and to determine the effect of low dose on blood flow estimates.

## 2. METHODS

### Animal Model and CT Image Acquisition

The animal study was approved by the Institutional Animal Care and Use Committee. We used a porcine ischemic model (3 pigs, weight: 40kg) with a percutaneous balloon-induced ischemia guided by fractional flow reserve (FFR) [8]. In this animal model, a balloon catheter is introduced in the femoral artery and implanted in the left anterior descending (LAD) coronary artery. An FFR wire is placed with one pressure sensor proximal to the balloon,  $P_p$ , and one sensor distal to the balloon,  $P_d$ . The extent of ischemia is monitored in real-time by the FFR measurement,  $FFR = P_d/P_p$  [19]. The balloon is inflated to induce the desired level of stenosis as determined by FFR, with targeted values of  $FFR=0.7$  and  $FFR<0.3$  in this study. Once the balloon and FFR wire have been placed, the animal is

moved from the surgical suite to a clinical CT scanner. Inside the CT scan room, the balloon is inflated to obtain the desired stable FFR value and dynamic CTP scans are performed.

Dynamic contrast-enhanced myocardial CT perfusion scans were performed on a Philips iCT system. A bolus injection of 20mL contrast (Omnipaque 350) followed by 20mL saline at 5mL/s was used. Scans were started 4s after contrast injection. A total of 50 scans at 100kVp/100mAs were obtained with 8cm coverage and 23mSv effective dose. To minimize cardiac motion effects, partial scan acquisitions (0.18s, 240deg) and ECG-gating were used at 45% phase (end systole). Respiratory motion was suppressed by turning off the ventilator during scans. Typical scan times were approximately 30s.

### Simulation of low dose CTP scans and image reconstruction

To compare reconstruction algorithms for dose reduction we used a projection-based low dose simulation tool which accounts for photon statistics and electronic noise in energy-integrating CT systems [18]. The sinogram at low dose is computed according to equation (1) below (see [18] for more details):

$$\hat{s}_{\alpha \rightarrow \beta, c} = A \frac{\alpha - \beta}{\alpha} P\left(\frac{\beta}{\alpha - \beta} \frac{\hat{s}_{\alpha, c}}{A}\right) + D_c \sqrt{1 - \frac{\beta^2}{\alpha^2}} \quad (1)$$

where  $\hat{s}_{\alpha \rightarrow \beta, c}$  is the output low dose sinogram value,  $\alpha$  is the original tube current,  $\beta$  is the simulated low tube current such that  $\beta < \alpha$ ,  $\hat{s}_{\alpha, c}$  is the original sinogram value,  $P(\cdot)$  is the Poisson noise sampling function,  $D_c$  is the total detector gain which includes scintillator, photodiode, and electronic, sample of detector noise, and  $A$  is the total detector gain which includes scintillator, photodiode, and electronic gains. The simulator operates on sinogram data from CT scans after beam hardening and scatter corrections have been applied. Photon and electronic noise are added to the projections to achieve the defined low dose. Physical detector noise samples are used for  $D_c$ . It is important to include detector noise in dose reduction studies, as the effect becomes increasingly significant at low exposures. We used the original 100mAs scans to simulate low dose scans at 75mAs, 50mAs, and 25mAs, corresponding to  $\alpha = 556mA$  and  $\beta = 418mA$ ,  $278mA$ , and  $139mA$ , respectively.

The high and low dose CT perfusion scans were reconstructed with IMR, iDose<sup>4</sup>, and FBP, giving a total of 12 image datasets per physical scan (4 dose levels, 3 reconstructions). All reconstructions used a 2mm slice increment with 3mm reconstructed slice thickness (1mm overlap), the same 120mm field of view centered on the heart at 512×512 resolution, and 35–36 slices/scan (7.0–7.2cm reconstructable data due to partial scan). Reconstruction kernels and settings were selected for the relatively low-resolution task of myocardial perfusion. A prototype IMR reconstructor was used with the cardiac L2 setting [20]. The iDose<sup>4</sup> Level 4 reconstruction used a standard adult body kernel [11]. FBP used a standard adult body kernel. All dose levels were reconstructed with these settings and compared in subsequent analyses. Since all images were derived from the same high dose raw data, any artifacts or physiologic variation will be the same and only the noise due to dose reduction or reconstruction will vary. An example of the low dose simulation and reconstruction workflow is shown in Fig. 1.

## Dynamic CT Perfusion Processing and blood flow quantification

An in-house developed dynamic CTP analysis pipeline was used to process each set of images. The pipeline includes beam hardening reduction, registration, partial scan artifact reduction, LV myocardial segmentation, and blood flow quantification [8]. For each condition (dose level and reconstruction), the following processing steps are taken. After image reconstruction, image-based beam hardening reduction is applied. The dynamic image volumes are registered using free form deformation with normalized mutual information. Axial images are then reformatted into the short axis view. Temporal-bilateral filtering (TBF) is used to reduce partial scan fluctuations. Semiautomated segmentation is performed to generate myocardial masks for blood flow quantitation. Blood flow quantification is performed using model-independent deconvolution with Tikhonov-regularized singular value decomposition (SVD).

In the deconvolution process, we computed blood flow,  $F$ , as the maximum value of the flow-scaled impulse response function,  $FR(t)$ . Using the measured left ventricle (LV) cavity arterial input concentration,  $C_a(t)$ , and the LV myocardial tissue concentration,  $C_t(t)$ , we obtained  $FR(t)$  by deconvolution of the following relation

$$C_t(t) = C_a(t) \otimes FR(t) \quad (2)$$

which comes from the indicator-dilution theory [21] where  $\otimes$  denotes the convolution operation. We discretized equation (2) into the form of a matrix equation,  $Ax = b$ , where  $A$  is generated from  $C_a(t)$ ,  $b$  is the tissue concentration curve  $C_t(t)$ , and  $x$  is the impulse response function,  $FR(t)$  [22, 23]. We used the block-circulant formulation of  $A$  to account for time delay between  $C_a(t)$  and  $C_t(t)$  [22]. Using SVD, we decompose  $A$  such that  $A = U\Sigma V^T$ , where  $\Sigma$  is a diagonal matrix of singular values,  $\sigma_i$  in non-increasing order, and  $U = [u_1, u_2, \dots, u_N]$  and  $V = [v_1, v_2, \dots, v_N]$  are unique orthogonal matrices [22, 23]. The solution of the matrix equation is given by

$$x = \sum_{i=1}^N \left( \frac{u_i^T b}{\sigma_i} \right) v_i. \quad (3)$$

However, the matrix  $A$  is ill-conditioned and thus very sensitive to noise in the measured data. To obtain a numerically stable solution, we use Tikhonov regularization which modifies equation (3) above to

$$x = \sum_{i=1}^N \left( \frac{\sigma_i^2}{\sigma_i^2 + \lambda^2} \right) \left( \frac{u_i^T b}{\sigma_i} \right) v_i \quad (4)$$

effectively reducing the weights on small singular values, particularly where  $\sigma \ll \lambda$ . The effect of this regularization can be quite pronounced and proper selection of the regularization parameter value is important, as this will directly impact blood flow measurements. The effect of  $\lambda$  on the solution  $FR(t)$  is illustrated in Fig. 2. Because flow is obtained by a maximum operation on the tissue impulse response function, this means that flow over-estimation is possible from noise spikes in the non- or under-regularized solutions,

but flow can also be under-estimated from over-regularization. Therefore, it is desirable that a reconstruction technique is not highly susceptible to noise. In this study, we set  $\lambda = 0.09$  and compare blood flows from each condition.

### Image quality assessment of static and dynamic CTP images

Static CTP images obtained at peak myocardial contrast were analyzed for image quality. Axial slice images distal to the balloon-induced stenosis were analyzed after beam hardening reduction and registration. Peak myocardial contrast was found by drawing large ROIs in healthy and ischemic myocardium, computing the mean healthy and ischemic HU, and taking the difference for each time point. The scan at which this difference was greatest gives the peak myocardial contrast, and was used for the subsequent static CTP analysis. Images from each condition (dose and reconstruction) were qualitatively compared for the ability to identify ischemia and quantitatively compared using SNR and CNR. SNR was calculated from a large ROI in healthy myocardium. CNR was quantified as the difference between the mean HU in the healthy ROI and a large ischemic LAD ROI, since the aim in static CT perfusion is typically to visually compare the enhancement in two territories (healthy and at-risk). Both metrics are given below:

$$SNR = \frac{\mu_{healthy}(HU)}{\sigma_{healthy}(HU)}; \quad CNR = \frac{\mu_{healthy}(HU) - \mu_{ischemic}(HU)}{\sqrt{\frac{1}{2}(\sigma_{healthy}^2(HU) + \sigma_{ischemic}^2(HU))}}. \quad (5)$$

Since the images are derived from the same data set, the ROIs are perfectly co-registered between conditions enabling direct comparisons between SNR and CNR. Higher SNR and CNR values indicate better image quality for static CTP.

Blood flow maps from dynamic CTP were similarly evaluated for image quality and flow quantification. Blood flow maps for each condition were generated using the short axis view after all CTP pipeline processing. Qualitative assessment was used to compare the ability to identify ischemia. Quantitative assessment included the comparison of mean blood flow, flow-SNR (fSNR), and flow-CNR (fCNR). The value of fSNR was computed from a large ROI in healthy myocardium. The value of fCNR was computed using the the same large healthy ROI and a large ischemic ROI. The two metrics are given below:

$$fSNR = \frac{\mu_{healthy}(Flow)}{\sigma_{healthy}(Flow)}; \quad fCNR = \frac{\mu_{healthy}(Flow) - \mu_{ischemic}(Flow)}{\sqrt{\frac{1}{2}(\sigma_{healthy}^2(Flow) + \sigma_{ischemic}^2(Flow))}}. \quad (6)$$

Again, since the images are derived from the same original scan, these values can be directly compared between dose and reconstruction conditions. Higher fSNR and fCNR values indicate better image quality for dynamic CTP. A consistent blood flow measurement at low dose as compared to high dose indicates the reconstruction algorithm is suitable for dynamic CTP.

### 3. RESULTS

A comparison of static CTP images at peak contrast for qualitative assessment is shown in Fig. 3. A severe ischemic case ( $\text{FFR} < 0.3$ ) is shown. Ischemia can be identified with all reconstructions at 100mAs. At 25mAs, FBP is heavily degraded by noise and iDose<sup>4</sup> is also degraded whereas IMR still shows ischemia comparable to 100mAs FBP. We found iDose<sup>4</sup> at 50mAs to be visually comparable to 100mAs FBP.

Fig. 4 shows the quantitative image quality measures from static CTP images of severe ischemia ( $\text{FFR} < 0.3$ ). Both SNR and CNR decrease as dose is reduced for all reconstructions. For any given dose level, SNR and CNR are highest for IMR and lowest for FBP. From these measures, IMR at 25mAs and iDose<sup>4</sup> at 50mAs are comparable to FBP at 100mAs.

Fig. 5 shows blood flow maps from the dynamic CTP data with a moderate stenosis ( $\text{FFR} \sim 0.7$ ). Visually, we observe that blood flow maps are comparable between all reconstructions at 100mAs. At low dose, FBP highly over-estimates flow, and the ischemia is much harder to detect (undetectable in the case shown in Fig. 5). Similarly, iDose<sup>4</sup> appears to lose ischemic contrast and over-estimate flow at 25mAs, but we found that visual comparison at 50mAs was comparable to 100mAs FBP. Flow maps from IMR at 25mAs were slightly degraded from 100mAs, but overall were quite comparable to the high dose results. Thus for moderate stenosis, ischemia was sometimes undetectable at low dose for FBP and iDose<sup>4</sup>.

A comparison of blood flow as a function of dose for each reconstruction is shown in Fig. 6. As dose is reduced in FBP, blood flow increases. Similarly, blood flow in iDose<sup>4</sup> also increased at low dose, but at a lower rate than FBP, and is reasonably consistent down to 50mAs. This effect is much reduced in IMR, which gives only slightly greater blood flow estimates at 25mAs compared to 100mAs. These effects can be observed in both the ischemic and healthy territories.

The effect of reduced dose on the impulse response functions from FBP and IMR is shown in Fig. 7. In FBP, as dose is reduced, fluctuations in the flow-scaled tissue impulse response function increase, leading to over-estimation of blood flow and greater overall flow map noise. However in IMR, these fluctuations at low dose are much reduced, yielding more consistent flow measurements.

The comparison of blood flow image quality metrics is given in Fig. 8. For all reconstructions, we see only a small decrease in flow-SNR at reduced dose, whereas flow-CNR decreases dramatically for FBP and iDose<sup>4</sup>. This suggests that flow-CNR is a better metric for assessment of flow map quality as compared to flow-SNR. This is due to the over-estimation of mean blood flow which causes flow-SNR to appear high even at low dose. Comparing flow-CNR values, IMR at 25mAs is comparable to FBP at 100mAs and iDose<sup>4</sup> at 50mAs. Flow-CNR is highest for IMR at all dose levels and lowest for FBP.



## 4. DISCUSSION

Using a preclinical model and simulated low dose scans, we found that advanced iterative reconstruction, such as IMR, can enable dose reductions in static and dynamic myocardial CT perfusion. In static CTP images, we found that IMR reconstructed images have the highest SNR and CNR at all dose levels, owed to the significant noise reduction. IMR at 25mAs, iDose<sup>4</sup> at 50mAs, and FBP at 100mAs gave similar qualitative identification of ischemia as well as SNR and CNR values. Similarly, for dynamic CTP, we found that blood flow images obtained at 25mAs IMR, 50mAs iDose<sup>4</sup>, and 100mAs FBP are of similar quality for qualitative detection of moderate ischemia and have comparable flow-CNR values. These results suggest dose reductions of 75% for advanced IR and 50% for hybrid IR in static and dynamic CTP as compared to conventional FBP reconstructions.

We studied the effect of dose reduction on blood flow quantification. As dose is reduced, the amount of image noise in the reconstructions increases. This leads to greater noise in the arterial input function and tissue time attenuation curve. This increase in noise produces fluctuations in the deconvolved tissue impulse response function which can be large. Because of the maximum operation to obtain the blood flow from the flow-scaled impulse response function, these fluctuations tend to produce over-estimates in blood flow. Reconstruction algorithms that reduce the level of image noise are therefore less susceptible to this over-estimation effect. This explains the greater increase in blood flow measurements at low dose in FBP whereas iDose<sup>4</sup> and IMR are less affected. For this reason, the aggressive noise reduction in advanced iterative reconstructions is well-suited for myocardial CTP due to its consistent HU measurements at low dose. Additionally, perfusion is a relatively low-resolution task which typically compares coronary territories rather than small structures, so aggressive noise reduction is sensible.

In this work, we used a constant Tikhonov regularization parameter in order to compare noise effects across dose and reconstruction. As one would expect, the addition of noise to signals in the SVD computation without additional regularization will lead to noise in the deconvolved output. To account for this affect, some have proposed adaptive Tikhonov parameter selection processes, such as the L-curve criterion, which balances low noise in the solution with data consistency [24, 25]. We applied this technique in our study on myocardial perfusion imaging with Spectral Detector CT [23]. However, searching for the optimal regularization parameter can be computationally intensive and difficult for the wide range of noise values in FBP reconstruction. As such, the low variability in image noise across dose for advanced IR will likely still provide more consistent results with the adaptive regularization techniques.

There are several limitations in this work. First, we have performed these analyses on simulated low dose scans. While this enables a direct comparison of image noise effects on CTP independent of artifacts or physiology, the dose reductions found here may be higher than in real scans. However, the dose simulation tool used here is closer to physical low dose acquisitions than alternatives, especially with the inclusion of detector noise. Second, we do not validate flow values in this work. Absolute flow accuracy is less of a concern in this work as we examined the relative effects of noise in each reconstruction. In previous studies,

we compared to FFR values for relative flow validation. For future absolute flow validation, we are developing a high-resolution fluorescent microsphere technique using an imaging cryo-microtome, or cryo-imaging. Third, there are residual beam hardening and partial scan artifacts in the CTP data reported here which impact absolute flow quantification. Hardware solutions exist which reduce these artifacts: fast gantry rotations enable full scan acquisitions to avoid partial scan artifact with little cardiac motion blur, and recent dual energy or spectral CT systems much reduce the level of beam hardening artifact [7, 23]. Similarly, there are potential algorithmic corrections which may reduce the effect of these artifacts and benefit the many existing systems in the field [9, 26].

The use of advanced IR can complement a number of other dose reduction strategies. Tube current reduction combined with advanced IR is one method for dose reduction which we explored here. Adaptive temporal sampling in dynamic CTP can reduce the number of scans to those most important for flow quantification [27]. Similarly, non-uniform tube currents may be used to acquire low noise images at sensitive time points [27]. Lastly, using prior knowledge of the stenosis location from coronary CT angiography, the x-ray beam may be collimated to a smaller z-coverage to evaluate a smaller portion of coronary territory. A combination of these strategies with advanced IR suggest that dynamic CTP at  $<5.8\text{mSv}$  may be possible, well below the current clinical standard SPECT of  $10\text{mSv}$  [12].

We found that advanced iterative reconstructions such as IMR can reduce x-ray dose in static and dynamic myocardial CT perfusion in a preclinical ischemic model. Using simulated low dose CTP scans, we found dose reductions of 75% for IMR and 50% for iDose<sup>4</sup>, corresponding to dynamic CTP protocols of  $5.8\text{mSv}$  and  $11.5\text{mSv}$ , respectively. These dose reductions make CT a feasible imaging modality for myocardial perfusion imaging as well as a clinical tool for rapid, noninvasive diagnosis of coronary artery disease.

## 5. CONCLUSION

We found that advanced iterative reconstruction (IMR, Philips Healthcare, Cleveland, OH) enables significant dose reductions in myocardial CT perfusion, reducing dose from  $23\text{mSv}$  in FBP protocols to  $5.8\text{mSv}$  with IMR. Static CTP images reconstructed with IMR showed the best image quality according to SNR and CNR. CTP images at  $25\text{mAs}$  with IMR were comparable to FBP images at  $100\text{mAs}$ . At high dose, all reconstructions measured similar blood flow from dynamic CTP. At low dose, IMR measured similar blood flow and had comparable flow-CNR to high dose FBP whereas FBP and iDose<sup>4</sup> became unstable and systematically over-estimated blood flow. This systematic over-estimation at low dose is due to noise effects in the deconvolution calculation, to which IMR is more resistant at low dose. In closing, we found that advanced iterative reconstruction, such as IMR, can enable significant dose reductions in dynamic CTP without sacrificing blood flow measurement quality.

## ACKNOWLEDGEMENTS

This research project was sponsored by NIH R01 EB004070, an NIBIB T32EB007509 training grant award to Brendan Eck, an Ohio Third Frontier research grant, *Cardiac Perfusion with Computed Tomography*, from the state of Ohio to CWRU, University Hospitals of Cleveland, Philips Healthcare, and a research contract from Philips



Healthcare to CWRU. Thanks go to Steve Schomisch and Cassie Koch of the CWRU Animal Resource Center and Scott Esposito at University Hospitals for their assistance with the preclinical experiments.

## 7. REFERENCES

- [1]. Hoffmann U, Nagurney JT, Moselewski F et al., "Coronary multidetector computed tomography in the assessment of patients with acute chest pain," *Circulation*, 114(21), 2251–2260 (2006). [PubMed: 17075011]
- [2]. Ehara M, Surmely J-F, Kawai M et al., "Diagnostic accuracy of 64-slice computed tomography for detecting angiographically significant coronary artery stenosis in an unselected consecutive patient population comparison with conventional invasive angiography," *Circulation Journal*, 70(5), 564–571 (2006). [PubMed: 16636491]
- [3]. Tonino PA, Fearon WF, De Bruyne B et al., "Angiographic versus functional severity of coronary artery stenoses in the FAME study: fractional flow reserve versus angiography in multivessel evaluation," *Journal of the American College of Cardiology*, 55(25), 2816–2821 (2010). [PubMed: 20579537]
- [4]. Berman DS, Hachamovitch R, Shaw LJ et al., "Roles of nuclear cardiology, cardiac computed tomography, and cardiac magnetic resonance: assessment of patients with suspected coronary artery disease," *Journal of Nuclear Medicine*, 47(1), 74–82 (2006). [PubMed: 16391190]
- [5]. Huber AM, Leber V, Gramer BM et al., "Myocardium: dynamic versus single-shot CT perfusion imaging," *Radiology*, 269(2), 378–386 (2013). [PubMed: 23788717]
- [6]. Rocha-Filho JA, Blankstein R, Shturman LD et al., "Incremental Value of Adenosine-induced Stress Myocardial Perfusion Imaging with Dual-Source CT at Cardiac CT Angiography 1," *Radiology*, 254(2), 410–419 (2010). [PubMed: 20093513]
- [7]. So A, Lee T-Y, Imai Y et al., "Quantitative myocardial perfusion imaging using rapid kVp switch dual-energy CT: preliminary experience," *Journal of cardiovascular computed tomography*, 5(6), 430–442 (2011). [PubMed: 22146502]
- [8]. Fahmi R, Eck BL, Vembar M et al., "Dynamic CT myocardial perfusion imaging: detection of ischemia in a porcine model with FFR verification." 903800-903800-10 Proc. SPIE Medical Imaging 2014 (2014).
- [9]. Alessio A, So A, and Lee T-Y, "Image-based Partial Scan Artifact Reduction for Dynamic Contrast Enhanced CT," *Radiological Society of North America 2013 Scientific Assembly and Annual Meeting*, <<http://archive.rsna.org/2013/13029053.html>> (2013).
- [10]. So A, and Lee T-Y, "Quantitative myocardial CT perfusion: a pictorial review and the current state of technology development," *Journal of cardiovascular computed tomography*, 5(6), 467–481 (2011). [PubMed: 22146506]
- [11]. Gramer B, Muenzel D, Leber V et al., "Impact of iterative reconstruction on CNR and SNR in dynamic myocardial perfusion imaging in an animal model," *European radiology*, 22(12), 2654–2661 (2012). [PubMed: 22752461]
- [12]. Cerqueira MD, Allman KC, Ficaro EP et al., "Recommendations for reducing radiation exposure in myocardial perfusion imaging," *Journal of nuclear cardiology*, 17(4), 709–718 (2010). [PubMed: 20503120]
- [13]. Funama Y, Taguchi K, Utsunomiya D et al., "Combination of a low tube voltage technique with the hybrid iterative reconstruction (iDose) algorithm at coronary CT angiography," *Journal of computer assisted tomography*, 35(4), 480 (2011). [PubMed: 21765305]
- [14]. Utsunomiya D, Weigold WG, Weissman G et al., "Effect of hybrid iterative reconstruction technique on quantitative and qualitative image analysis at 256-slice prospective gating cardiac CT," *European radiology*, 22(6), 1287–1294 (2012). [PubMed: 22200900]
- [15]. Fahmi R, Eck BL, Vembar M et al., "Dose reduction assessment in dynamic CT myocardial perfusion imaging in a porcine balloon-induced-ischemia model." 903305-903305-11 Proc. SPIE Medical Imaging 2014 (2014).
- [16]. Mehta D, Thompson R, Morton T et al., "Iterative model reconstruction: simultaneously lowered computed tomography radiation dose and improved image quality," *Med Phys Int J*, 2(1), 147–55 (2013).

- [17]. Katsura M, Matsuda I, Akahane M et al., "Model-based iterative reconstruction technique for radiation dose reduction in chest CT: comparison with the adaptive statistical iterative reconstruction technique," *European radiology*, 22(8), 1613–1623 (2012). [PubMed: 22538629]
- [18]. Žabi S, Wang Q, Morton T et al., "A low dose simulation tool for CT systems with energy integrating detectors," *Medical physics*, 40(3), 031102 (2013). [PubMed: 23464282]
- [19]. De Bruyne B, and Sarma J, "Fractional flow reserve: a review," *Heart*, 94(7), 949–959 (2008). [PubMed: 18552231]
- [20]. Funama Y, Taguchi K, Utsunomiya D et al., "Image quality assessment of an iterative reconstruction algorithm applied to abdominal CT imaging," *Physica Medica*, 30(4), 527–534 (2014). [PubMed: 24662097]
- [21]. Zierler K, "Indicator dilution methods for measuring blood flow, volume, and other properties of biological systems: a brief history and memoir," *Annals of biomedical engineering*, 28(8), 836–848 (2000). [PubMed: 11144667]
- [22]. Fieselmann A, Kowarschik M, Ganguly A et al., "Deconvolution-based CT and MR brain perfusion measurement: theoretical model revisited and practical implementation details," *Journal of Biomedical Imaging*, 2011, 14 (2011).
- [23]. Fahmi R, Eck BL, Fares A et al., "Dynamic Myocardial Perfusion in a Porcine Balloon-induced ischemia model using a prototype Spectral Detector CT." *Proc. SPIE Medical Imaging 2015* (2015).
- [24]. Koh T, and Hou Z, "A numerical method for estimating blood flow by dynamic functional imaging," *Medical engineering & physics*, 24(2), 151–158 (2002). [PubMed: 11886835]
- [25]. Jerosch-Herold M, Swingen C, and Seethamraju RT, "Myocardial blood flow quantification with MRI by model-independent deconvolution," *Medical physics*, 29(5), 886–897 (2002). [PubMed: 12033585]
- [26]. Kyriakou Y, Meyer E, Prell D et al., "Empirical beam hardening correction (EBHC) for CT," *Medical physics*, 37(10), 5179–5187 (2010). [PubMed: 21089751]
- [27]. Modgil D, Bindschadler MD, Alessio AM et al., "Adaptive sampling of CT data for myocardial blood flow estimation from dose-reduced dynamic CT." *Proc. SPIE Medical Imaging 2014* (2015).

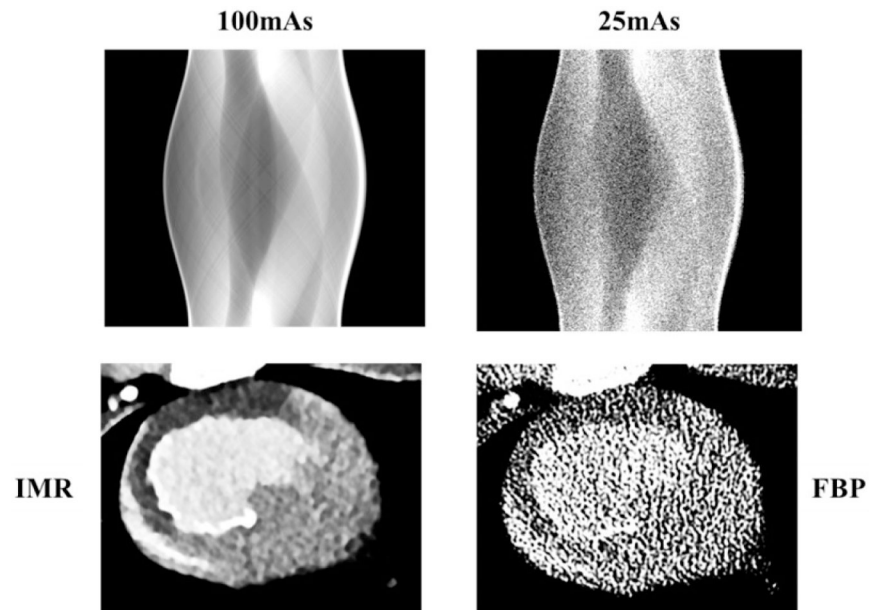


**Figure 1. Simulation of low dose CTP scans from high dose scans.**

Noise is added to the original projections (top-left) to obtain the desired dose level (top-right). Projections are reconstructed with FBP, iDose<sup>4</sup>, and IMR for each dose level giving 12 conditions in total. Static and dynamic CTP comparisons are made between the reconstructed images. Shown is a representative case with a high dose (100mAs) axial slice IMR image (bottom-left) and the corresponding low dose (25mAs) FBP image (bottom-right).

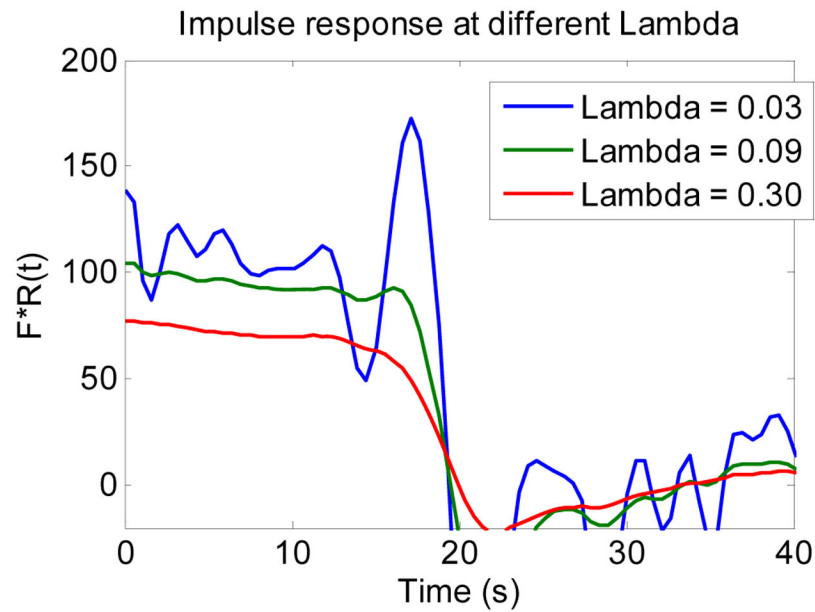


**Figure 2. Impulse response function obtained from SVD with different regularization parameter values.**

The flow-scaled impulse response function from regularized deconvolution is shown with different values of the regularization parameter,  $\lambda$ . Blood flow is obtained by taking  $F = \max(FR(t))$ . With a small regularization parameter, noise produces large fluctuations which lead to over-estimation of blood flow (blue). With over-regularization, the tissue response signal is damped and flow is under-estimated (red). Proper selection of lambda balances these two extremes (green).

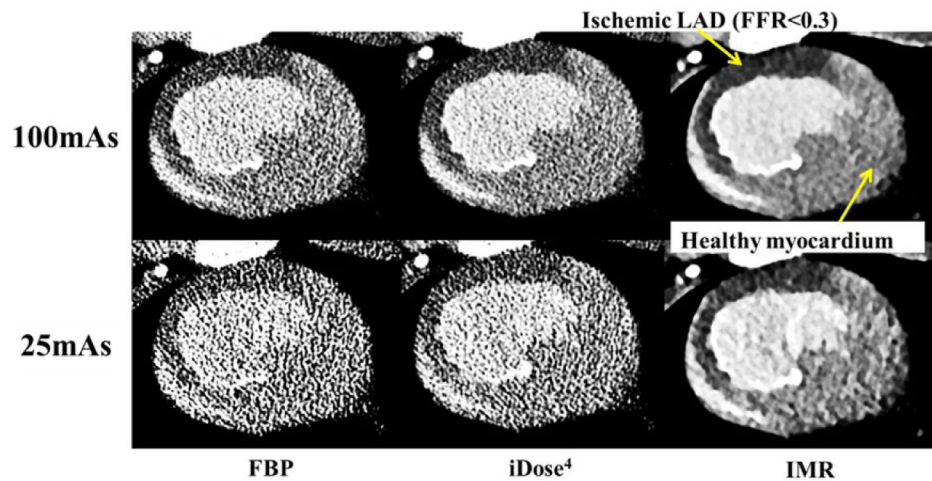


**Figure 3. Qualitative comparison of static CTP images at peak contrast.**

Axial CTP images for a severe ischemia ( $\text{FFR} < 0.3$ ) are shown at peak myocardium contrast. The ischemic territory is indicated and can be seen visually as a dark band of the LAD territory. The healthy myocardium is the brighter, contrast enhanced tissue. At high dose (top row), ischemia is clearly identified for all reconstructions, but at low dose (bottom row) the noise degrades the image, severely in FBP and less with  $\text{iDose}^4$ , making the ischemia difficult to detect. Detection of ischemia is comparable between IMR at low dose and FBP at high dose. All images shown at  $\text{WW}=150$ ,  $\text{WL}=85$ .

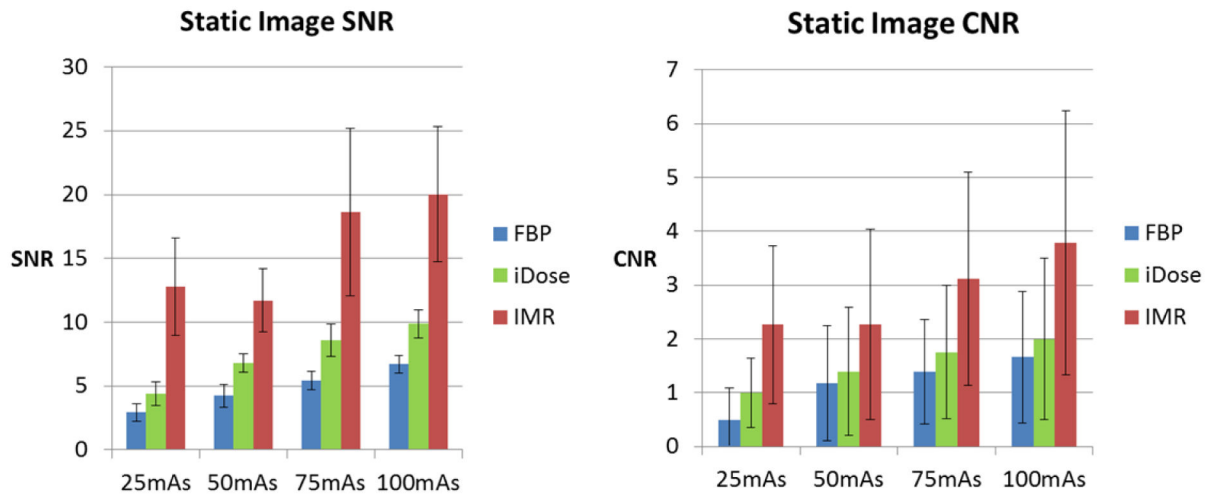


**Figure 4. Quantitative image quality comparison for dose and reconstruction conditions (FFR<0.3).**

Image SNR and CNR is highest for IMR at all dose levels and lowest for FBP. SNR and CNR for IMR at 25mAs and iDose<sup>4</sup> at 50mAs are comparable to FBP at 100mAs.



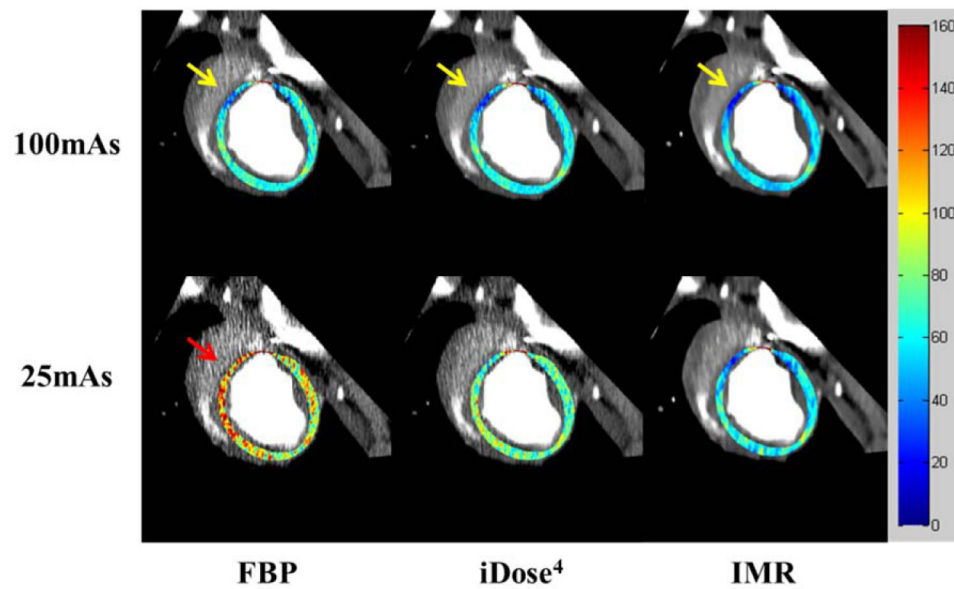


**Figure 5. Blood flow maps from high and low dose dynamic CTP.**

Blood flow maps for a moderate LAD territory ischemia ( $FFR \sim 0.7$ ) are overlaid on static short axis view CTP images. The top row shows FBP, iDose<sup>4</sup>, and IMR reconstructions at full dose, 100mAs/23mSv. Ischemia can be seen on the antero-septal wall for all reconstructions at 100mAs (yellow arrow). The bottom row shows blood flow obtained at low dose, 25mAs/5.8mSv. Blood flow greatly increases in FBP due to noise, causing the ischemic territory to appear highly perfused (red arrow). Blood flow at 25mAs increases with iDose<sup>4</sup> to a lesser extent. Blood flow from IMR at 25mAs is consistent with 100mAs flow maps. Ischemia is difficult to detect at 25mAs with FBP and iDose<sup>4</sup>.

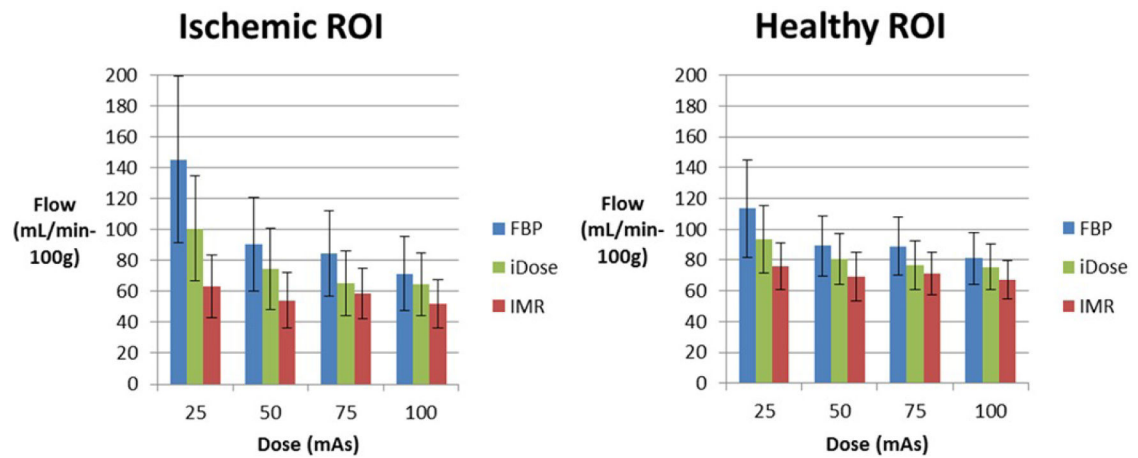


**Figure 6. Blood flow obtained from corresponding myocardial ROIs for dose and reconstruction conditions (FFR~0.7).**

Blood flow increases for FBP as dose is reduced in both healthy and ischemic ROIs.

Similarly, blood flow from iDose<sup>4</sup> also increases especially below 50mAs. IMR is more consistent across this dose range yielding comparable flow values at 25mAs as at 100mAs.

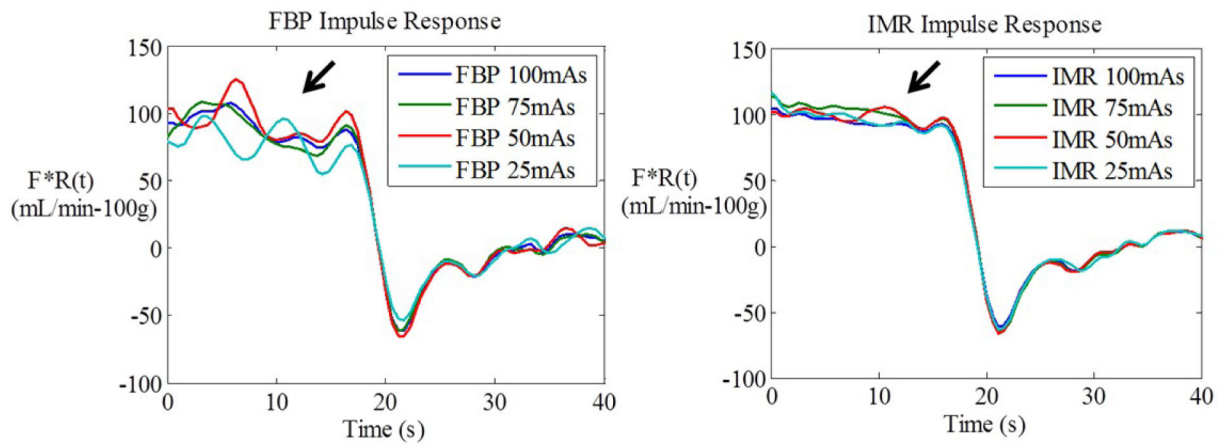


**Figure 7. Tissue impulse response function ( $F \cdot R(t)$ ) for FBP and IMR at different x-ray dose levels.**

For the same ROI, fluctuations in FBP increase more dramatically as dose is reduced than in IMR (marked by arrows).

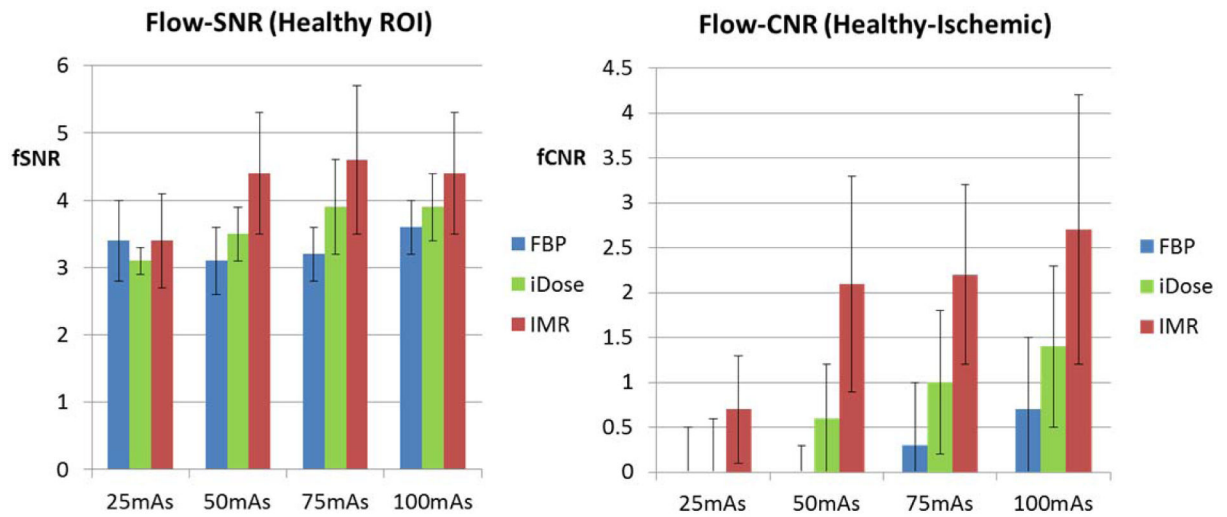


**Figure 8. Image quality comparison of blood flow images from dynamic CTP for a moderate ischemia (FFR~0.7).**

Flow-SNR appears relatively constant for all conditions due to the over-estimation of blood flow. Flow-CNR decreases as dose is reduced causing FBP and iDose<sup>4</sup> to become undetectable at 25mAs whereas IMR at 25mAs is comparable to FBP at 100mAs.